Kinetics of Protein Adsorption and Desorption on Surfaces with Grafted Polymers

Fang Fang,* Javier Satulovsky,† and Igal Szleifer*
*Department of Chemistry, Purdue University, West Lafayette, Indiana; and †Department of Cell Biology and Physiology, Washington University School of Medicine, St. Louis, Missouri

ABSTRACT The kinetics of protein adsorption are studied using a generalized diffusion approach which shows that the time-determining step in the adsorption is the crossing of the kinetic barrier presented by the polymers and already adsorbed proteins. The potential of mean-force between the adsorbing protein and the polymer-protein surface changes as a function of time due to the deformation of the polymer layers as the proteins adsorb. Furthermore, the range and strength of the repulsive interaction felt by the approaching proteins increases with grafted polymer molecular weight and surface coverage. The effect of molecular weight on the kinetics is very complex and different than its role on the equilibrium adsorption isotherms. The very large kinetic barriers make the timescale for the adsorption process very long and the computational effort increases with time, thus, an approximate kinetic approach is developed. The kinetic theory is based on the knowledge that the time-determining step is crossing the potential-of-mean-force barrier. Kinetic equations for two states (adsorbed and bulk) are written where the kinetic coefficients are the product of the Boltzmann factor for the free energy of adsorption (desorption) multiplied by a preexponential factor determined from a Kramers-like theory. The predictions from the kinetic approach are in excellent quantitative agreement with the full diffusion equation solutions demonstrating that the two most important physical processes are the crossing of the barrier and the changes in the barrier with time due to the deformation of the polymer layer as the proteins adsorb/desorb. The kinetic coefficients can be calculated a priori allowing for systematic calculations over very long timescales. It is found that, in many cases where the equilibrium adsorption shows a finite value, the kinetics of the process is so slow that the experimental system will show no adsorption. This effect is particularly important at high grafted polymer surface coverage. The construction of guidelines for molecular weight/surface coverage necessary for kinetic prevention of protein adsorption in a desired timescale is shown. The time-dependent desorption is also studied by modeling how adsorbed proteins leave the surface when in contact with a pure water solution. It is found that the kinetics of desorption are very slow and depend in a nonmonotonic way in the polymer chain length. When the polymer layer thickness is shorter than the size of the protein, increasing polymer chain length, at fixed surface coverage, makes the desorption process faster. For polymer layers with thickness larger than the protein size, increases in molecular weight results in a longer time for desorption. This is due to the grafted polymers trapping the adsorbed proteins and slowing down the desorption process. These results offer a possible explanation to some experimental data on adsorption. Limitations and extension of the developed approaches for practical applications are discussed.

INTRODUCTION

Flexible polymer molecules grafted to surfaces or interfaces impose a steric barrier that can be tuned depending upon the polymer molecular weight, surface coverage, and type of chemical structure (1–3). These interactions are widely used in colloidal stabilization (4–6) and in the last few years have found application on the development of biocompatible materials and drug carriers (7–25). The basic idea is that the grafted polymer layer prevents nonspecific adsorption of proteins on the surface of the biocompatible material or drug carrier, reducing the immunological response (7,8,15,26–29). The understanding of the kinetics of protein adsorption and its reduction/prevention by grafted polymer layers is therefore very important for the design of materials interacting with biological systems. In this work we present a thorough theoretical study of the kinetics of protein adsorption on surfaces with grafted polymers, which complements our earlier work on both the thermodynamics and kinetics of protein adsorption (30–34).

Adsorption of proteins on surfaces is a complex process that involves very large energy scales and the ability of the proteins to change their conformation upon contact with the surface (26,35–38). Moreover, the timescale of the adsorption process can be very long and in many cases the adsorption is irreversible (31,33,39–41). It is important to differentiate between the equilibrium isotherms and the kinetics of the adsorption process. This is an important difference both in the practical applications of protein adsorption (or prevention of it) and in the fundamental studies of the understanding of the adsorption process. For example, in the design of biocompatible materials to be used for artificial organs it is important to completely prevent adsorption of proteins. Thus, thermodynamic control is necessary, meaning that for the given conditions, the equilibrium amount of proteins adsorbed on the surface is zero. On the other hand, drug carriers need to survive in the blood stream for the time

Submitted October 27, 2004, and accepted for publication June 2, 2005.

Address reprint requests to I. Szleifer, Dept. of Chemistry, Purdue University, 560 Oval Dr., West Lafayette, IN 47907. Tel.: 765-494-5255; Fax: 765-494-5489; E-mail: igal@purdue.edu.

0006-3495/05/09/1516/18 $2.00

doi: 10.1529/biophysj.104.055079

necessary to deliver the drug to its target. In this case, control of the kinetics of adsorption, so that it is delayed beyond the timescale for drug delivery, is the necessary design criteria.

During the last few years we have developed and applied a molecular theoretical approach to study the thermodynamics and kinetics of protein adsorption on surfaces with and without grafted polymers (21,24,30–33,42–45). The predictions from the theory are in excellent quantitative agreement for the adsorption isotherms of lysozyme and fibrinogen on surfaces with short- (31) and long-grafted polyethylene oxide (PEO) chains (21,32). In all these cases we studied systems in which the reduction of protein adsorption is due to the steric repulsion induced by the polymer layer, i.e., by flexible polymer and not by chemical modification of the surface, as in the case of high density self-assembled monolayers with functional end-groups (46). We have found that the grafted polymer layers properties that are optimal for thermodynamics control are different than those controlling the kinetic process (31,33). For example, for thermodynamic control of protein adsorption the polymer surface coverage is the most important factor in determining the reduction of protein adsorption (30). These predictions have been confirmed by experimental observations (16,47). For the kinetics of adsorption, though, we have predicted a very strong effect on molecular weight; however, its role for the equilibrium isotherms is only secondary (31,33).

In this article we present a kinetic theory that borrows from our previous work (31) and the insights learned from the theory of Halperin (48) and we develop a computational feasible molecular approach that enables the study of the whole kinetic process explicitly accounting for the deformation of the polymer-protein layer as the adsorption process takes place. The basic idea of the approach is to use the physical insights learned from the generalized diffusion approach to determine what the relevant steps are in the kinetic process. Then, we use the theoretical ideas of the Kramer-like approach developed by Halperin together with our molecular theory to construct a kinetic model that enables the study of both adsorption and desorption processes.

The next section, Molecular Theory, starts with a review of the generalized diffusion approach and the molecular theory that serves as basis for the kinetic approach. After that, we present the kinetic theory used, with examples of the kinetics of adsorption and desorption as a function of the grafted polymer chain length and surface coverage; this is then followed by our concluding remarks.

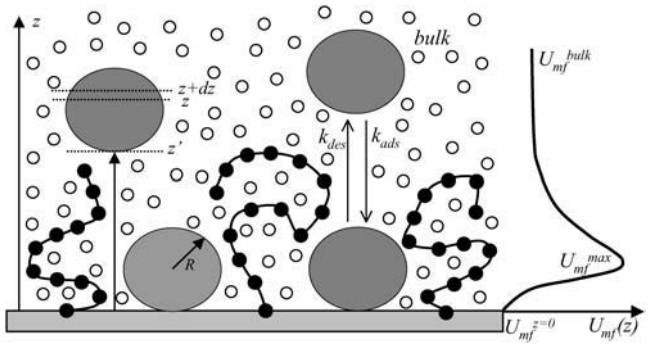

FIGURE 1 Schematic representation of the system containing proteins in their native conformation dissolved in a low molecular-weight solvent, and in contact with a surface with grafted polymers. The large solid circles are the proteins and the small open circles are the solvent molecules. The strings of small solid circles, tethered to the surface, represent the grafted polymers. The z direction is defined perpendicular to the surface. The position of a protein, z', refers to the lowest point of the protein, whereas the volume that a protein contributes to z refers to the volume that the protein occupies between z and $z + dz$. The two rate coefficients represent the kinetic processes involved in the adsorption of proteins onto the surface with grafted polymers. The right of the figure represents schematically the potential of mean-force felt by the adsorbing/desorbing proteins (see text).

MOLECULAR THEORY

The system of interest here is composed of a surface of total area A spanning the x, y plane. The surface has N_g polymer molecules grafted at one of their ends (see Fig. 1). Each polymer has n_g segments, each of length l. The polymer-modified surface is put, at time $t = 0$, in contact with a solution containing proteins dissolved in water. The protein solution is characterized by a bulk density $\rho_{p,bulk}$ or equivalently a chemical potential $\mu_{p,bulk}$. When the surface is put in contact with the solution the proteins ''feel'' anisotropic interactions, induced by the presence of the surface, which are the driving forces for the adsorption process.

The basic idea to determine the time- and distance-dependent interactions between the surface and the proteins is to take advantage of the very different timescale for the diffusion of the protein as compared to the fast local motions of the polymer monomers and the solvent molecules. Therefore, we can consider that for each configuration in space of the proteins, the polymer and solvent can equilibrate around the larger, slower, particles. This assumption is common to our generalized diffusion approach that we present here and the kinetic model in next section. We start reviewing the generalized diffusion approach followed by the free energy functional molecular theory approach.

In this work we concentrate our attention only on cases in which the protein does not change its conformation upon adsorption. The generalization of the theory to more general cases has been presented elsewhere for bare surfaces (33). It will be shown in future work for surfaces with grafted polymers.

GENERALIZED DIFFUSION APPROACH (GDA)

The basic assumptions of separation of timescale present a natural scenario for the use of dynamical self-consistent theory or the dynamical density functional approach (31,49–51). This is effectively what we call the generalized diffusion approach (GDA), when the free energy used is from our

molecular theory (33). We write a time-evolution equation for the density profile of the proteins with a diffusion equation of the form

$$\frac{\partial \rho_p(z;t)}{\partial t} = D_p \frac{\partial}{\partial z}\left[\rho_p(z;t)\frac{\partial}{\partial z}\mu_p(z;t)\right], \quad (1)$$

with D_p the diffusion coefficient of the proteins. (Please note that, for simplicity, we assume that the diffusion coefficient is independent of position. The reason is that the kinetic slowdown induced by the interactions, through the chemical potential gradients, is the dominant effect in the cases of interest here.) The time- and position-dependent chemical potential is defined as

$$\mu_p(z;t) = \frac{\delta W/A}{\delta \rho_p(z;t)}. \quad (2)$$

W/A represents the free energy density (per unit area) of a system of frozen configuration of the proteins. This means it is the minimal free energy with respect to the polymers and the solvent for the given distribution of proteins. It is convenient to write the chemical potential as the sum of an ideal term and a potential of mean-force $U_{mf}(z;t)$, i.e., the nonideal contribution. Then

$$\mu_p(z;t) = k_B T \ln \rho_p(z;t) + U_{mf}(z;t), \quad (3)$$

where k_B is the Boltzmann constant and T is the absolute temperature. Using the potential of mean-force definition, Eq. 3, on the diffusion equation, Eq. 1, we obtain

$$\frac{\partial \rho_p(z;t)}{\partial t} = D_p\left[\frac{\partial^2 \rho_p(z;t)}{\partial z^2} + \frac{\partial}{\partial z}\rho_p(z;t)\frac{\partial U_{mf}(z;t)}{\partial z}\right]. \quad (4)$$

The first term is the ideal diffusion, whereas the second represents the motion due to the interactions between the proteins and all the other molecules in the system, including the surface. Consider for example the case in which, at time $t = 0$, a solution with homogeneously distributed proteins is put in contact with the surface. The main driving force for adsorption has to be the potential of mean-force, since there is no gradient of density. However, because proteins adsorb, the two terms contribute until the chemical potential (due to the balance of density and potential of mean-force) becomes constant and the new equilibrium with the adsorbed proteins is reached. Clearly, if there is a strong attraction between the proteins and the surface the new equilibrium corresponds to an inhomogeneous distribution of proteins, due to the anisotropic interaction potential that results from the presence of the surface.

At this point we should remark that the concept of chemical potential and potential of mean-force are defined as generalizations of the equilibrium (true thermodynamic) properties (52,53). We refer to the time- and distance-dependent quantities in the same way as in the equilibrium cases. That is, they are formally defined in the same way, but do not correspond to the quantities for when the system is in true thermodynamics equilibrium. Instead, they correspond to the minimal free energy under the constraint of frozen distribution of protein as given at that time by the dynamic equation.

FREE ENERGY FUNCTIONAL MOLECULAR THEORY

The understanding of the adsorption process from one equilibrium state to a new one, requires the variation of the free energy, W. To this end, we use the molecular theory that we originally developed to treat the structural and thermodynamic properties of tethered polymer layers and later generalized to treat protein adsorption on surfaces with and without grafted polymers (3,24,30–33,42–45,54–57) . The basic idea is to write the free energy as a functional of the density of proteins and the conformational probability distribution of the grafted polymer chains and the proteins. To write the free energy we consider each molecular species exactly (within the chosen model to describe the molecular system) in terms of the intramolecular and surface interactions. The intermolecular interactions are considered within a mean-field approximation.

The presence of the surface induces an inhomogeneous distribution of all the molecular species. Therefore, the mean-field felt by the molecules in each of their conformations is a function of the spatial distribution of its units and the average distribution of all the other molecular species. For simplicity we consider that the only inhomogeneous direction is the one perpendicular to the surface, i.e., the z direction.

We derive the free energy for a simple case of a mixture of polymers and proteins in which the solvent is equally good for both molecular species. Further, we assume that the protein can only be in its native conformation and does not change its conformation upon adsorption to the surface. The generalization to the cases in which conformational changes upon adsorption are considered (34), as well as different intermolecular interactions, has been treated elsewhere (30).

The free energy per unit area of the equilibrium combined protein-grafted polymer system is given by

$$\begin{aligned}\frac{\beta W}{A} = {} & \sigma \sum_{\gamma} P_g(\gamma) \ln P_g(\gamma) \\ & + \int_0^{\infty} \rho_p(z)[ln\, \rho_p(z) v_s - 1 + \beta U_{ps}(z) - \beta \mu_p] dz \\ & + \int_0^{\infty} \rho_s(z)[\ln \rho_s(z) v_s - 1] dz, \end{aligned} \quad (5)$$

where $\beta = 1/k_B T$. The first term represents the conformational entropy of the tethered polymers, where $\sigma = N_p/A$ is the polymer surface coverage and $P_g(\gamma)$ (pdf) is the probability of finding a grafted polymer in conformation γ. The second term is the protein contribution, including:

1. A z-dependent mixing (translation) entropy with $\rho_p(z)$ representing the protein density profile; v_s is the solvent volume which is used as the unit of volume throughout.

2. The distance-dependent bare protein-surface attraction, $U_{ps}(z)$.
3. The chemical potential term to ensure equilibrium with the bulk, i.e., constant chemical potential of the proteins at all z with $\mu_p = \mu_{p,bulk}$.

The last term represents the z-dependent mixing entropy of the solvent where $\rho_s(z)$ is the solvent density at z.

Inspection of Eq. 5 shows that the intermolecular repulsive interactions are not included. We assume that the repulsive interactions are of the excluded volume type and thus we include them through packing constraints. That is, at each distance z from the surface the volume accessible to the molecules in the layer between z and $z + dz$ is completely occupied by a sum of contributions from the polymers, the proteins, and the solvent molecules. This is expressed in the form

$$\sigma\langle v_g(z)\rangle + \int \rho_p(z')v_p(z;z')dz' + \phi_s(z) = 1, \qquad (6)$$

where the first term is the volume fraction of polymers in layer z, with $\langle v_g(z)\rangle = \sum P(\gamma)v_g(z;\gamma)$ being the average volume that a grafted polymer occupies at z. The second term is the volume fraction of protein. This term includes the integral over z' since we need to consider the contribution to the volume at z from proteins everywhere. The term $v_p(z;z')$ is the volume that a protein with its point of closest distance at z' contributes to z (see Fig. 1). The last term is the solvent volume fraction with $\phi_s(z) = \rho_s(z)v_s$. The packing constraint explicitly includes the size and shape of each of the molecular species in the system, as well as the spatial distribution of volume for each polymer conformation.

We now can find the explicit functional form of the pdf of chain conformations and the density profiles of proteins and solvent by performing a functional minimization of the free energy with respect to the polymer pdf, protein, and solvent density profiles subject to the packing constraints. The minimization is carried out by introducing Lagrange multipliers, $\beta\pi(z)$, associated with the packing constraints, to yield

$$P_g(\gamma) = \frac{1}{q_g}e^{-\int \beta\pi(z)v_g(z;\gamma)dz}, \qquad (7)$$

for the pdf of chain conformations, with q_g being the grafted polymers' partition function (normalization constant that ensures $\sum_\gamma P_g(\gamma) = 1$), and

$$\rho_p(z) = e^{\beta\mu_p}e^{-\beta U_{ps}(z) - \int \beta\pi(z')v_p(z';z)dz'}, \qquad (8)$$

for the protein density profile. The equation for the protein density profile ensures that the chemical potential of the protein is the same at all z as required for thermodynamic equilibrium.

Finally, the solvent density profile is given by

$$\phi_s(z) = e^{-\beta\pi(z)v_s}. \qquad (9)$$

The physical meaning of the Lagrange multipliers can be seen in the expression of the solvent volume fractions profile (Eq. 9). They represent the local osmotic pressures. They actually measure the work to replace one unit of volume of solvent by one of polymer or protein. As discussed elsewhere (3,30,33, 34), the lateral pressures are a measure of the average repulsive interaction at distance z from the surface. The numerical values of the lateral pressures are determined by replacing the explicit expressions of the polymer pdf, Eq. 7, the protein density profile, Eq. 8, and the solvent density profile, Eq. 9, into the constraint equation, Eq. 6. The resulting equations require, as input, the single chain conformations of the polymer chains; the protein volume distribution; the polymer surface coverage; and the protein chemical potentials. For details on how the equations are solved numerically, see the Appendix.

At this point it is instructive to look at the expression of the protein chemical potential. At equilibrium it is given from Eq. 8 by

$$\beta\mu_p = \ln\rho_p(z) + \beta U_{mf}(z), \qquad (10)$$

where we have defined the potential of mean-force $U_{mf}(z)$ by

$$\beta U_{mf}(z) = \beta U_{ps}(z) + \int \beta\pi(z')v_p(z';z)dz'. \qquad (11)$$

This quantity represents the effective interaction between a protein at z and the surface, averaged over all the degrees of freedom of the other molecules in the system. This quantity, actually its time-dependent counterpart, plays a key role in the kinetics of adsorption (see Eq. 2, above).

The free energy functional and the pdf and density profiles just derived correspond to the equilibrium state of the system since they are found by the total minimization of the free energy functional. To determine the time-dependent quantities necessary to solve the generalized diffusion equation, Eq. 4, we use the separation of timescales mentioned above and consider a free energy with the same functional form as Eq. 5 but with a major modification. Following the assumption that the local motion of the polymers and that of the solvent are much faster than the proteins' motion, we can consider that for each given density profile of the proteins, the free energy contribution of the solvent and polymers is minimized. Therefore, we write the time-dependent free energy in the form

$$\begin{aligned}\frac{\beta W(t)}{A} = {} & \sigma\sum_\gamma P_g(\gamma;t)\ln P(\gamma;t) \\ & + \int_0^\infty (\phi_s z;t)[\ln\phi_s(z;t) - 1]dz \\ & + \int_0^\infty \rho_p(z;t)[ln\,\rho_p(z;t) - 1 + U_{ps}(z)]dz, \end{aligned} \qquad (12)$$

where the protein component is written without a chemical potential term; the time-dependent polymer pdf and solvent profile are obtained by minimization of the free energy; and the protein density profile is fixed, and is given by the dynamic equation, Eq. 4.

We need to minimize the free energy with respect to the pdf and the solvent density profile subject to the packing constraints. Following the same lines as in the equilibrium case, we introduce a time-dependent Lagrange multiplier, $\beta\pi(z;t)$, which is associated with the time-dependent packing constraints. For the pdf and solvent-density profile expressions (identical to Eqs. 7 and 9, respectively), this leads to $\pi(z)$ being replaced by $\pi(z;t)$. For the determination of the lateral pressures, the main difference between the equilibrium and nonequilibrium cases is that, in the equilibrium case, the protein density profile is obtained in the minimization process and is therefore an explicit function, $\pi(z)$; but in the nonequilibrium case, $\rho_p(z;t)$ is an input. In general, the input comes from the diffusion equation. However, this does not have to be the case, as will be discussed in detail in the description of the kinetic approach.

The next step is to determine the time- and z-dependent chemical potential of the protein. This is obtained as a straightforward generalization of the equilibrium quantity (see Eqs. 10 and 11),

$$\beta\mu_p(z,t) = \left(\frac{\delta W(t)/A}{\delta\rho_p(z;t)}\right), \tag{13}$$

to obtain

$$\beta\mu_p(z;t) = \ln\rho_p(z;t) + \beta U_{ps}(z) + \int \beta\pi(z',t)v_p(z';z)dz', \tag{14}$$

and thus the time-dependent potential of mean-force is given by

$$U_{mf}(z;t) = \beta U_{ps}(z) + \int \beta\pi(z';t)v_p(z';z)dz', \tag{15}$$

in analogy to the equilibrium amount. Note that the bare surface-protein interaction is time-independent. All of the time-variation arises from the intermolecular interactions as expressed in the lateral repulsions $\pi(z;t)$, which result from the changes in the packing of the protein-polymers as the proteins move toward the adsorbing surface.

To solve the equilibrium and kinetics of protein adsorption we need to define the model system for the protein and the polymers. For the protein we use a very simple model that mimics the properties of lysozyme. We assume that the protein is spherical with a radius $R_p = 1.5$ nm. Furthermore, for $U_{ps}(z)$, we use the potential calculated from atomistic simulations by Lee and Park (35) for lysozyme with polyethylene solid surfaces (see Fig. 2 below). For simplicity, we do not allow for conformational changes of the protein upon adsorption, and leave that for future work. For the polymer conformations, we use a rotational isomeric state model (58) in which each bond is allowed to have three isoenergetic states. This model is closely related to the one we have used to model PEO chains and the predictions are in excellent agreement with experimental observations

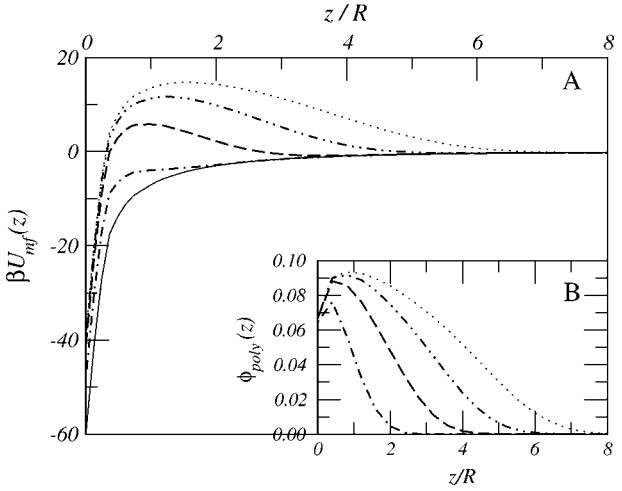

FIGURE 2 (*A*) The initial potential of mean-force for different chain lengths: $n_g = 0$ (*bare surface*, *solid line*); $n_g = 25$ (*dot-dashed line*); $n_g = 50$ (*long-dashed line*); $n_g = 75$ (*double-dot-dashed line*); and $n_g = 100$ (*dotted line*). The surface coverage is $\sigma l^2 = 0.01$. (*B*) The inset presents the corresponding polymer volume fraction profiles at $t = 0$.

(21,31,32,59). For each chain length that we study we use up to 2×10^6 randomly generated self-avoiding polymer conformations. From each conformation γ generated we obtain $v_g(z;\gamma)$, the volume that a chain in conformation γ has in the volume spanned between z and $z + dz$. These volume distributions are the input to solve the constraint equation, Eq. 6. Note that the set of conformations has all type of distributions of segments, $v_g(z;\gamma)$, including highly stretched chains and mushroom-like conformations. The pdf determines the relative weight of each conformation for each different case and for different times. (The Appendix outlines how the equations are solved by discretization of the z direction; for more detail on the technical aspects for the equilibrium and dynamic solutions, see Refs. 21, 30, 31, 33, and 34.) In all the results presented below, we denote the dimensionless densities given by the product ρv_s simply by ρ. To convert this quantity to the experimentally reported units of ng/cm^2 for lysozyme, one needs to multiply our reported values by 26,394. Otherwise, multiplying the reported values by 150 provides the area fraction occupied by the proteins.

REPRESENTATIVE RESULTS FOR GDA

The kinetics of protein adsorption is strongly affected by polymer-chain length. We have discussed these differences of molecular weight effects on the thermodynamics and kinetics of protein adsorption in early work (31). However, we find it important to highlight the main points again here as they help in the understanding of the kinetic theory and results developed below. The kinetic process that we study starts from a homogeneous solution of protein, $\mu_p(z) = \mu_{p,}$ bulk for all z, that at time $t = 0$ is brought into contact with

a layer of pure solvent of thickness δ that has a solid surface located at $z = 0$. The surface may have grafted polymers in it at surface coverage σ and the polymer chain length is n_g. The presence of the surface induces an interaction field in the z direction that generates gradients of chemical potential in the protein. These manifest themselves in varying potentials of mean-force, that at time $t = 0$ represent the driving force of the proteins, together with the gradient of the protein density, to adsorb on the surface. Fig. 2 shows the potentials of mean-force at time $t = 0$ for a variety of polymer chain lengths, all at the same surface coverage.

In the case of *no grafted polymers*, the potential is purely attractive and it is given by $U_{ps}(z)$. The presence of the grafted polymers introduces a repulsion whose range is equal to the thickness of the tethered layer (see *inset* of Fig. 2 for the polymer density profiles). For long enough polymers a repulsive barrier appears whose strength and position is a function of the polymer chain length. The amount of protein adsorbing at equilibrium depends on the potential of mean-force at contact. Even though the value of the potential at contact varies with the amount of proteins adsorbed (see below), the variation of $U_{mf}(z = 0; t = 0)$ with polymer chain length shows the same dependence as the equilibrium amount of proteins adsorbed (30).

The kinetics of adsorption depends upon the timescale required by proteins to reach the surface. In the case of purely attractive potentials, as for no polymer and $n_g = 25$ on Fig. 2, the initial adsorption will be very fast and determined by the time that it takes the proteins to reach the range of the interactions. In this regime the surface acts as a strong attractive sink to the proteins. For the other cases shown, however, the initial adsorption is determined by the time that it takes the proteins to cross the repulsive barrier presented by the polymer layer. We can see in the potentials that both the range and magnitude of the repulsion increases with polymer chain length. Therefore, the initial adsorption will be slower as the polymer-chain length increases. Also, we do not expect a fast regime in the initial adsorption whenever the potential of mean-force at $t = 0$ shows a maximum.

The solution of the generalized diffusion equation is obtained by integrating Eq. 1 with the initial condition mentioned above, and by using the potentials of mean-force presented in Fig. 2. However, once we integrate the first time-step the distribution of proteins changes and thus the potential of mean-force will also change. That is, it will correspond to the minimal free energy of the polymer-solvent mixture in the frozen *new* configuration of the proteins. Therefore, we expect the potentials of mean-force to be a strongly varying function of time. The complete kinetic behavior is presented in Fig. 3, where the amount of protein on the surface is plotted as a function of time. The figure shows the kinetics of adsorption for different cases: one in which there are no polymers grafted on the surface, with the rest representing surfaces with grafted polymers with the same surface coverage, but different molecular weights.

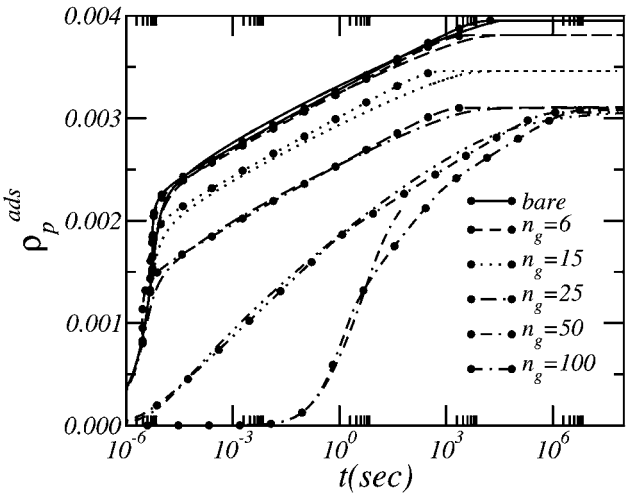

FIGURE 3 Variation of the amount of protein adsorbed as a function of time for surfaces with (and without) grafted polymers. The lines are the results from the generalized diffusion approach. The lines with symbols are the results from the kinetic theory approach. In all cases, $\sigma l^2 = 0.01$. The bulk protein volume fraction is $\phi_{p,\,bulk} = 0.001$. The different chain lengths are denoted in the figure.

The time-dependent adsorption for no-polymer on the surface and short-chain-length-grafted polymer shows a very fast early regime, in which the surface acts as a sink to the proteins due to the strong attractions between the surface and the proteins (see *potentials* in Fig. 2). After a certain amount of proteins adsorb, there is a very sharp slowdown, during which the kinetic process is dominated by barrier crossing. In the case of $n_g = 50$ we see in Fig. 2 the presence of a kinetic barrier even at the beginning of the adsorption process. Thus, Fig. 3 shows that the kinetics of adsorption does not have a fast regime but it is dominated at all times by barrier crossing. Actually, the height of the barrier and the range of the potential of mean-force change as the adsorption proceeds.

Fig. 4 shows the potential of mean-force for four different stages of the adsorption for $n_g = 50$. The height of the barrier increases, and it moves toward the surface as more proteins adsorb. Furthermore, the range of the repulsive interaction increases. This is the result of the deformation of the polymer layer as the proteins adsorb. The changes in the structure of the polymer layer and the volume fraction profile of the proteins at the same stages of the adsorption are also shown in Fig. 4. There is a clear push of the polymer segments close to the surface to move toward the solvent as the proteins adsorb. This is due to the need of the protein to have enough room on the surface to adsorb. The main message of the figure is that to properly describe the kinetic process, the deformation of the polymer-protein layer in the vicinity of the surface has to be taken into account. This is the contribution responsible for the very large variation of the potential of mean-force, and thus the rate of adsorption, with time.

Another important result from Fig. 4 is the profile of the protein volume fraction as a function of time. It is clear that

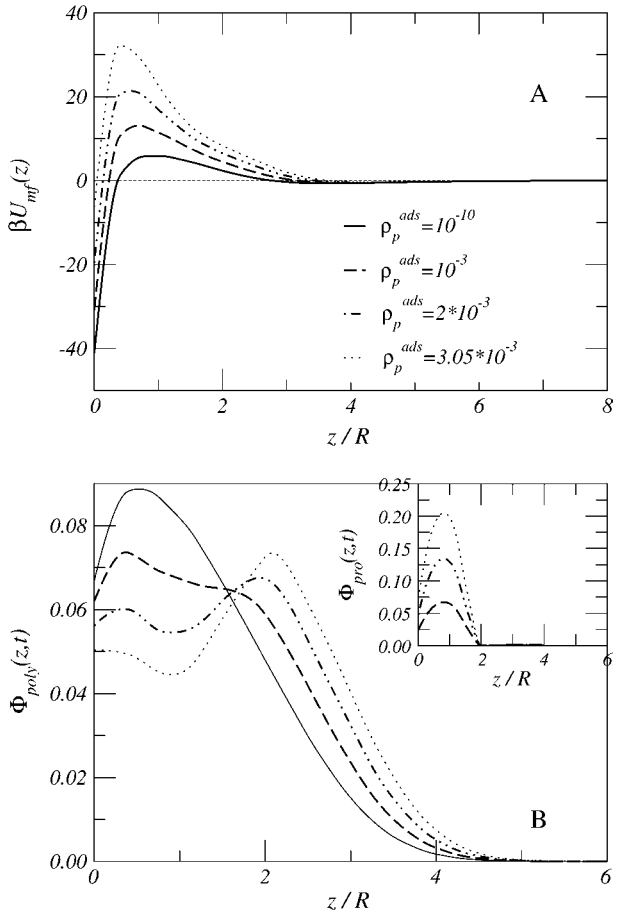

FIGURE 4 (*A*) The potential of mean-force at four different stages of the adsorption for the case of $n_g = 50$ shown in Fig. 3. (*B*) The volume fraction profile of grafted polymers, and the volume fraction profile of proteins (*inset*) corresponding to the same four stages shown in *A*.

the protein is found on the surface and then depleted from the other regions where the grafted polymer is, up to the bulk. This depletion is the result of the large effective repulsion felt by the proteins due to the grafted polymers. This two-state type of protein structure serves as the basis of the kinetic model that we present below. Based on this result, we can assume that the potential of mean-force, and in particular its maximum and value at contact, depends on the structure of the polymer-protein layer, when the proteins are only at the surface. Therefore, applying the free energy functional molecular theory approach, we can calculate the potentials of mean-force at all possible adsorbed densities from zero to the equilibrium value.

The description of the kinetics with the generalized diffusion model enables a rather detailed molecular description of the adsorption process with its associated structural changes. The problem is that the solution of the numerical equations is very demanding. First, the kinetic process requires the solution of the differential equations over 16 orders-of-magnitude in time. Second, at each time-step the determination of the chemical potential gradients is obtained by solving a set of coupled nonlinear equations with thousands of terms in each one, i.e., the constrained free energy minimization (see Appendix). The calculations for long chain lengths are practically impossible; as an example, the calculation for $n_g = 50$ presented in Fig. 3 takes many days of computer time. Moreover, there are cases where the time evolution is so slow that we cannot reach the equilibrium state (see, e.g., $n_g = 100$ in Fig. 3). Therefore, a more practical approach is needed, such as the one presented next.

KINETIC THEORY (KA)

Adsorption kinetics

We find the most problematic cases to solve with the above approach are those in which the barriers in the potential of mean-force are very high. These are also the cases in which we find a two-state protein distribution. Thus, we present a kinetic model in which the rate-determining step is the crossing of the barrier. This means that we look at a kinetic equation for the transition of proteins between the bulk and the adsorbed state given by

$$\frac{\partial \rho_{\mathrm{ads}}(t)}{\partial t} = k_{\mathrm{ads}}(t)\rho_{\mathrm{bulk}} - k_{\mathrm{des}}(t)\rho_{\mathrm{ads}}(t), \qquad (16)$$

where the first term on the right-hand side of Eq. 16 is the gain term associated with the increase of proteins on the surface due to the adsorption, and the second is the loss term due to the desorption of the proteins.

The adsorption and desorption are activated processes, as depicted qualitatively in Fig. 1. Therefore, the kinetic constants should have the form of

$$k_{\mathrm{ads}}(t) = k_1 e^{-\beta \Delta U_{\mathrm{ads}}(t)};\ k_{\mathrm{des}}(t) = k_2 e^{-\beta \Delta U_{\mathrm{des}}(t)}, \qquad (17)$$

where $\Delta U_{\mathrm{ads}}(t) = U_{\mathrm{mf}}(z = z^{\max};t) - U_{\mathrm{mf}}(bulk)$ is given by the difference in the potential of mean-force between the maximum of the barrier height and the bulk. The desorption Boltzmann factor, $\Delta U_{\mathrm{des}}(t) = U_{\mathrm{mf}}(z = z^{\max};t) - U_{\mathrm{mf}}(z = 0;t)$, is the difference between the potential at the maximum and that of the adsorbed state, i.e., the potential at contact with the surface (see Fig. 1).

Based on the full solution of the diffusion equation we assume that the potential of mean-force depends on the structure of the polymer-protein layer, when the proteins are only at the surface. Therefore, we can calculate the potentials of mean-force at all possible adsorbed densities from zero to the equilibrium value, meaning that we solve the equilibrium problem for the polymer-solvent with a fixed amount of protein ρ_{ads} on the surface. This allows us to calculate $U_{\mathrm{mf}}(z;\rho_{\mathrm{ads}})$, which we will use to determine the necessary energies for the Boltzmann factors in Eq. 17. Once we know the potential of mean-force as a function of ρ_{ads} and the distance from the surface, z, we can determine the height of the potential barrier and the potential at contact. Using our choice of zero for the potential in the bulk, $U_{\mathrm{mf}}(bulk) = 0$, we

know the three values of the potential of mean-force needed to calculate the rate coefficients.

The next step is to determine the preexponential factors in the rate coefficients. To this end we use the ideas of Halperin (48), who calculated the initial rate of adsorption of proteins on surfaces with grafted polymers using an extension of Kramer's theory of chemical reactions. We follow his approach but we explicitly include the time variation of the parameters determining the preexponential factor, thus allowing the complete treatment of the adsorption process from its initial condition up to the approach to equilibrium.

According to Kramer's theory, the preexponential factor is given by

$$k_1 = k_2 = \frac{D}{\alpha L} \tag{18}$$

(see derivation in the Appendix), where D is the diffusion constant; α is the width of the potential at a distance k_BT below the maximum; and L is the distance a protein in the bulk state has to travel to reach the barrier maximum, which can be approximated by the thickness of the polymer layer. Both α and L depend upon the molecular structure of the polymer layer. Therefore, they also depend on time through the changes in structure of the combined polymer-protein layer as a function of the amount of adsorbed proteins. As we have done with the barrier of the potential and its value at contact, we can determine α and L as a function of the amount of protein adsorbed. Thus, we can have the implicit dependence of the kinetic coefficients k_{ads} and k_{des} on time through their explicit dependence on the amount of protein adsorbed.

Note that the rate coefficients as defined fulfill microscopic reversibility at all times., i.e.,

$$\frac{k_{ads}(t)}{k_{des}(t)} = e^{-\beta(U_{mf}(z=0,t)-U_{mf}(bulk))}. \tag{19}$$

This result is consistent with our local equilibrium approximation. The symmetry arises from the approximations used in the derivation of the flux (see the Appendix for details and discussion). Other choices for the preexponential factors will not affect any of the results presented for the adsorption, since the kinetics of adsorption is dominated by the flux toward the surface. Furthermore, as it will be shown below, the excellent agreement between the predictions of the KA and the full GDA supports the validity of this approximation.

Fig. 4 demonstrates the very large changes that the polymer-protein layer structure undergoes through the adsorption process. Thus, it is clear that the proper quantification of the kinetic process requires the consideration of the explicit density-dependence, and thus the implicit time-dependence, of the quantities $U_{mf}(z = z_{max};\rho_{ads}(t))$, $U_{mf}(z = 0;\rho_{ads}(t))$, $\alpha(\rho_{ads}(t))$, and $L(\rho_{ads}(t))$. Examples of the first two quantities can be clearly seen in Fig. 4. We now discuss the four quantities in more detail, since they will provide insightful physical information on just what the roles of surface coverage and polymer-chain length are in the kinetic process.

Fig. 5 shows the maximum in the potential of mean-force as a function of the amount of adsorbed proteins for a variety of polymer-chain lengths. Also shown is the case of the bare surface. For short chain lengths (including the bare surface, $n_g = 0$), a barrier larger than the thermal energy appears only after a finite amount of proteins adsorb (see Fig. 5, *inset*, and the explanation below). However, for long enough chain length ($n_g \geq 40$ for the surface coverage shown in the figure), there is a barrier even when there are no proteins adsorbed. The variation of the maximum of the potential of mean-force with density reveals which one is the dominant contribution in determining the kinetic barriers: the polymer, the protein, or both. In all the regimes where the maxima are parallel, then, it is the protein that determines the variation of the potential. Note the reason that curves are parallel, and not identical, is that there is a background contribution of the polymer layer which is strongly dependent on chain length. For the regions in which the curves are not parallel, the polymer contribution is dominant. Thus, there is a very different maxima at low protein densities for the longest polymer chain lengths shown, where the polymer effect on the kinetics is large.

Interestingly, for the two longest chain lengths shown, the curves become identical for large amounts of proteins adsorbed. This implies that at these late stages of the adsorption the proteins see no difference between the two chain lengths. That the region close to the surface is basically identical, is because both chain lengths are long enough such that only

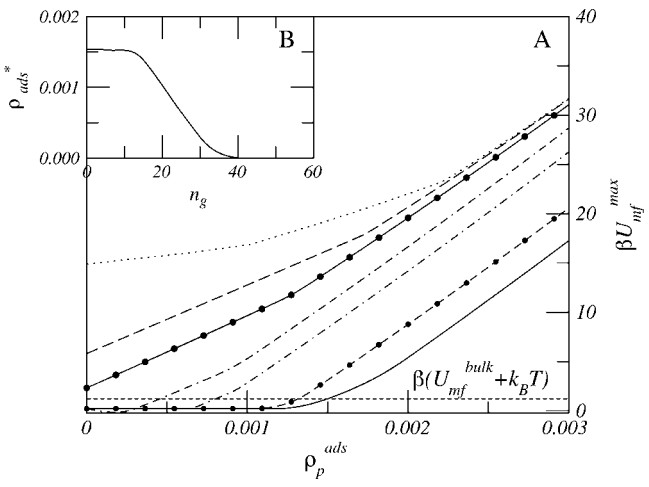

FIGURE 5 (*A*) The maximum in the potential of mean-force as a function of the density of proteins adsorbed on surfaces with grafted polymers for different chain lengths: $n_g = 0$ (*bare surface*, *solid line*); $n_g = 15$ (*large dots-dashed line*), $n_g = 25$ (*dot-dashed line*); $n_g = 30$ (*double-dash-dotted line*); $n_g = 40$ (*large dot-solid line*); $n_g = 50$ (*long-dashed line*); and $n_g = 100$ (*dotted line*). In all cases, $\sigma l^2 = 0.01$. The thin-dashed line at $\beta U^{max}_{mf} = \beta(U^{bulk}_{mf} + kT)$ marks the minimum potential that a kinetic barrier must present. (*B*) The inset presents the minimum density of protein that has to be adsorbed for the formation of a kinetic barrier as a function of grafted polymer-chain length.

a finite part of them is affected by the adsorption process. In other words, the degree of deformation is identical for both surfaces. Thus, we see a very interesting chain-length effect. First, when the polymer layer thickness is longer than the size of the protein, the *equilibrium* amount of proteins adsorbed is independent of molecular weight (34). Second, the initial rate of adsorption depends very strongly on the polymer-chain length; for example, the difference in the maximum of the potential of mean-force between $n_g = 50$ and $n_g = 100$ at $t = 0$ is 10 k_BT, implying a ratio of rate constants of the order of 10^{-5}. Third, once the adsorption is advanced, the maximum of the potential barrier for adsorption becomes identical for these chain lengths.

The kinetic approach cannot be directly applied to the initial adsorption kinetics if there is no barrier in the potential of mean-force at $t = 0$. This is the case for the polymer chains shorter than 35 segments, as shown in Fig. 5. In the absence of kinetic barriers, the solution of the GDA presented in the previous section is not computationally demanding. However, when the adsorption mechanism crosses over to be dominated by the crossing of the barrier, then we need to switch to the KA (see, e.g., $n_g = 25$ in Fig. 3). Thus, for practical purposes, it is important to have an amount of density adsorbed (as a function of polymer-chain length), showing a kinetic barrier larger than the thermal energy (see Fig. 5, *inset*). The use of this graph is that, for the surface coverage shown in the region below the curve, the kinetics of adsorption is obtained from the full solution of the GDA, whereas above the curve the practical approach is to use the KA. Clearly, the different regimes depend on the surface coverage of polymer and the specific protein studied. However, once those parameters are defined, we can calculate a curve, such as that shown in Fig. 5's inset, to find the proper approach to apply in each case.

Fig. 6 shows the values of the width of the steric barrier at $t = 0$ and at the end of the adsorption process as a function of grafted polymer-chain length. There is a strong dependence of α on n_g at $t = 0$ due to the specific structure of the polymer layer and its changes with the molecular weight of the polymer. The width of the potential barrier, however, is almost independent of the molecular weight of the polymer at the end of the adsorption process, and it is much smaller than its initial value. The data presented for the initial stage of adsorption in Fig. 6 presents the result for polymers shorter than 35 segments separately from the result for chains longer than 35 segments. The reason is that, below this molecular weight, there is no barrier in the potential of mean-force at $t = 0$ for the surface coverage shown (see Fig. 5, *inset*).

The very large change in α from the initial value to the end of the adsorption process is a reflection of the change in the shape of the potential as the adsorption process takes place. At the initial stages, the barrier is dominated completely by the grafted polymers. However, as the concentration of proteins on the surface increases, the barrier becomes more dominated by the contribution of the adsorbed proteins. Therefore,

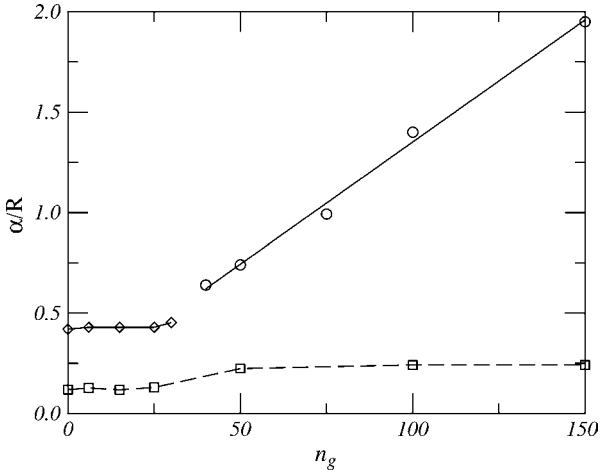

FIGURE 6 The width of the kinetic barrier, α, before adsorption (*solid line* with *circles*) and after adsorption (*dashed line* with *squares*) as a function of chain length for surfaces with grafted polymers at $\sigma l^2 = 0.01$. The solid line with diamonds represents the width of the kinetic barrier for the shorter polymer chains at the moment the kinetic barrier is just formed, i.e., $U_{mf}^{max} = U_{mf}^{bulk} + kT$, after some proteins have been adsorbed.

α becomes independent of the molecular weight of the polymer, because the maximum narrows, and its shape is due mostly to the protein and the polymer segments interacting with it, as discussed above.

The last variable that we need to discuss is the thickness of the polymer-protein layer L and its dependence on the amount of protein adsorbed. As it is well known from polymer brushes, the thickness of the layer varies linearly with the molecular weight of the polymer (1,57). What is interesting is that even after there is adsorption of proteins the change in the thickness of the layer is very small (results not shown). This is because the height of the polymer layer is not a very sensitive function of the local changes of the molecular organization in the region closed to the grafting surface. Thus, for practical purposes we can use the same L at all times; i.e., that for $t = 0$.

Desorption kinetics

We next consider the case in which, once the system reaches equilibrium, the protein solution in contact with the surface is washed-out and thus the adsorbed proteins in the grafted polymer layer are in contact with pure water. The equilibrium state will be such that all the proteins leave the surface since there is an infinite entropic gradient due to the zero concentration of proteins in solution. The kinetics of the process can, in principle, be studied with both the GDA and the KA. However, we found that the time evolution with the GDA is so slow that no calculations can be carried out. Therefore, we need to use the KA. We can write the kinetic equation for desorption in the form

$$\frac{\partial \rho_{ads}(t)}{\partial t} = -k_{des}(t)\rho_{ads}(t), \tag{20}$$

where there is no gain term because the solution is protein-free. The desorption rate coefficient is given by

$$k_{\mathrm{des}}(t) = \frac{D}{\alpha R} e^{-\beta \Delta U_{\mathrm{des}}} \tag{21}$$

(see derivation in the Appendix), where the energy difference is as given following Eq. 17, and we have used the Kramer approach for the preexponential factor. Note that instead of L we have R in the denominator of the preexponential factor. This is because the maximum of the potential of mean-force is located at a distance from the surface of the order of the protein size, as shown in Fig. 4. Thus, the desorption process measures the protein going from the surface to the maximum in the potential, i.e., a distance R from the surface. Interestingly, the width of the potential around the maximum for the desorption process is independent of chain length. However, it is a function of the amount of protein adsorbed and polymer surface coverage. The determination of α and ΔU_{des} as a function of time is obtained from the knowledge of these quantities as a function of the amount of density adsorbed, along the same lines as the KA is applied for the adsorption process (e.g., see Fig. 5).

Integration methodology

The equation for the adsorption and desorption kinetics, as derived from the KA, requires four parameters as a function of time. They are the potential of mean-force at contact, $U_{\mathrm{mf}}(z = 0, t)$; the maximal value of the potential of mean-force, $U_{\mathrm{mf}}(z = z^*,t)$; the width of the potential of mean-force of 1 $k_{\mathrm{B}}T$ below the maximum, $\alpha(t)$; and the thickness of the film, $L(t)$. The fifth quantity, $U_{\mathrm{mf}}(bulk)$, is independent of time. From the four quantities we have shown that the thickness of the film (or the radius of the protein for the desorption process) does not vary with time, and therefore we take its value at time $t = 0$. For the other three quantities we know their values as a function of the amount of protein on the surface, which we tabulate before starting the kinetic calculations. Thus, we start the integration at time $t = 0$ where we know all the necessary values and we integrate the kinetic equations one time-step. The integration gives the value of the density of adsorbed proteins at the new time. We use this density value to find the three parameters, from the tabulated values, and integrate the kinetic equations another step. We continue this iteration of finding the new density, obtaining the value of the kinetic coefficients at the new density and integrating a new time-step until we reach the equilibrium state.

REPRESENTATIVE RESULTS FOR KA

The first question that arises relates to the quality of the results obtained from the kinetic theory as compared to the diffusion approach. Fig. 3 shows the predicted kinetic curves for both cases. In the case of the KA, the curves are calculated in the valid region as denoted in the inset of Fig. 5. The agreement between the full calculations and the more approximate approach is very good. The shape of the adsorption curves and the magnitudes are very well reproduced for all grafted polymer-chain lengths and in the whole range of time in which a barrier is present. This implies that the physical mechanism for protein adsorption on surfaces with grafted polymers is indeed what we have assumed; that is, once there is a kinetic barrier, the time-determining step is that of crossing the barrier. However, it is imperative to explicitly include the variation of the parameters as the proteins adsorb to properly describe the whole kinetic process—i.e., the polymer-protein layer deformation determines the shape of the time-dependent adsorption.

It is important to emphasize the difference in the computational effort necessary to solve the KA as compared to the GDA. For the case of $n_{\mathrm{g}} = 50$ there is a factor of 10^6 between the two calculations. Furthermore, there are many cases in which the GDA needs to be integrated with a very small time-step, and therefore the calculations cannot be completed at all (see, e.g., the curve for $n_{\mathrm{g}} = 100$ in Fig. 3). However, for the KA, the calculations are very simple; in essence, for each time-step, the solution is that of a simple first-order differential equation.

The reliability of the results from the KA gives us confidence to apply it where the GDA is not practical due to the computational limitations. Thus, we now study the effect of polymer-chain length and surface coverage. Fig. 7 shows the kinetics of adsorption for three different surface coverages of polymers and three different chain lengths. The figure shows that increasing both the chain length and the surface coverage results in slower kinetics. Interestingly, as we have shown elsewhere (30,31,34), for the three chain lengths shown, the equilibrium adsorption is almost independent of polymer chain but depends on surface coverage. However, the kinetic process slows, by orders of magnitude, with both chain length and surface coverage.

The variation of the kinetic process with grafted poly mer-chain length is different for each of the three surface coverages shown. For the smallest surface coverage presented, there are large differences in the initial adsorption time; however, for the three chain lengths, the proteins reach their equilibrium-adsorbed amount at more or less the same time. For the two larger surface coverages, this is not the case. The longer the polymer-chain length, the slower the whole adsorption process becomes. Further, as the surface coverage increases, the differences at the latter stages of the adsorption process become larger.

As the surface coverage of grafted polymer increases, the chain molecules become more stretched. This results in several effects on the protein adsorption. First, the layer is more protein-resistant, because there is less room for the proteins to adsorb. Second, the barriers for adsorption become larger, and therefore display slower adsorption kinetics. Third,

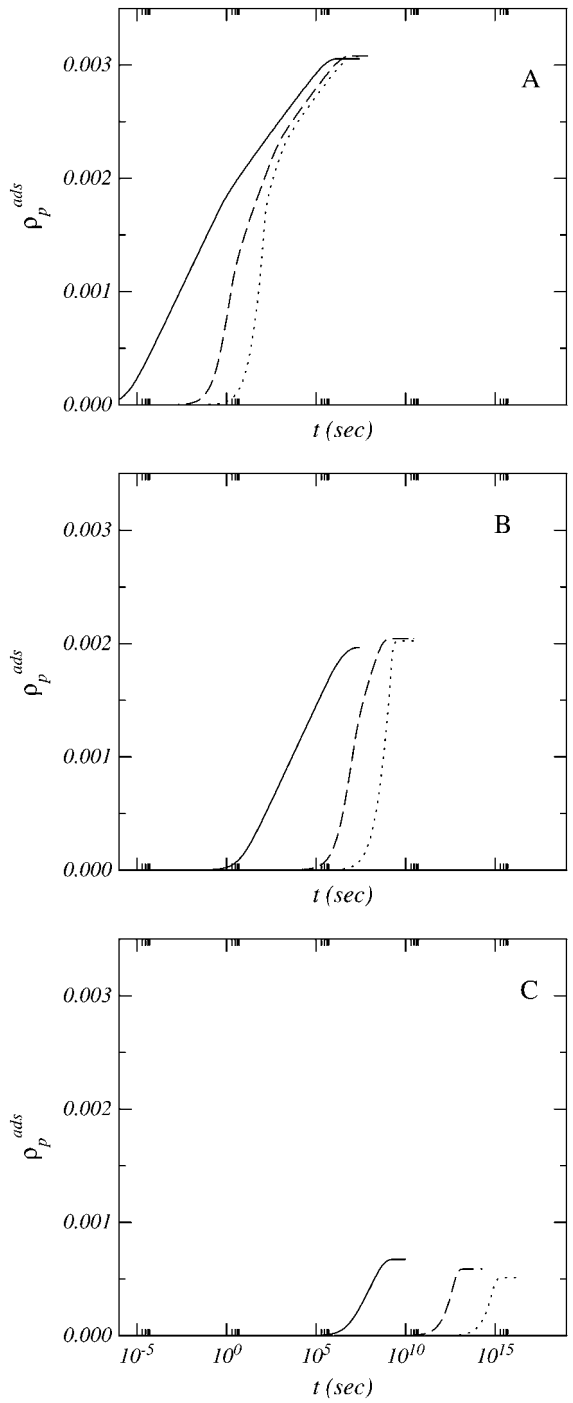

FIGURE 7 The amount of proteins adsorbed as a function of time for different grafted polymer-surface coverages: (*A*) $\sigma l^2 = 0.01$, (*B*) $\sigma l^2 = 0.02$, and (*C*) $\sigma l^2 = 0.03$. The different curves in each graph represent different chain lengths: $n_g = 50$ (*solid line*), $n_g = 100$ (*dashed line*), and $n_g = 150$ (*dotted line*). In all cases, the bulk protein-volume fraction is $\phi_{p,\,bulk} = 0.001$.

the polymer molecules have a large degree of stretching due to the interpolymer repulsions; therefore, the degree of polymer layer deformation upon protein adsorption is smaller than for lower σ. Thus, variation of the effect of polymer chain length on the kinetics as a function of time is much less pronounced at high σ than at lower surface coverage. The result is that the adsorption kinetics looks the same at different stages (for different chain lengths) and the lag between the curves is maintained throughout the adsorption. Then, we see that for $\sigma l^2 = 0.01$, there is a difference in the initial adsorption time of six orders-of-magnitude between $n_g = 50$ and $n_g = 100$, but less than one order-of-magnitude to reach equilibrium. On the other limit for $\sigma l^2 = 0.03$, we find a difference of seven orders-of-magnitude in time for chain lengths 50 and 100, which is maintained until the system reaches thermodynamics equilibrium.

The question that arises, however, is what is the significance of treating systems in which the equilibrium is reached in 10^{14} s, or equivalently, 10^6 years? The reason for showing these results is that unless we do the calculation we do not know the timescale for adsorption. The calculations with the KA are rather simple, and we can gain insights into why the timescale is so long and how chain-length variations have different behavior at different surface coverage. Further, if we just perform an equilibrium calculation we obtain that there is a finite adsorption even for $n_g = 150$ and $\sigma l^2 = 0.03$. This suggests that such a high surface coverage should not be enough, say, for a biocompatible material to completely prevent protein adsorption. However, the timescale for even the initial adsorption is predicted to be so large that for all practical purposes, this coating of the surface should completely prevent protein adsorption for all relevant experimental times.

In reality, we do not need to calculate the whole kinetic process, to see that the timescale of the adsorption process is infinitely slow for practical purposes. This is one of those cases where the initial adsorption time is all we need. If the time for initial adsorption is short enough within the experimental timescale, then we can perform the whole calculation. To show the dependence of timescales on molecular weight and surface coverage, Fig. 8 displays the maximum of the potential of mean-force before any adsorption take place as a function of polymer surface coverage for three different molecular weights of polymer. The maximum is found to have a close-to linear dependence on surface coverage, and the slopes depend on polymer molecular-weight.

The timescale for adsorption is determined by the rate coefficient k_{ads}; thus, we also need the dependence of α and L, actually the product αL, as a function of surface coverage (also shown in Fig. 8). The thickness of the polymer layer increases with surface coverage, whereas the width of the potential decreases. The decrease in α is faster than the increase in the thickness, and therefore we find that there is an overall decrease of the product with surface coverage. This implies that the effect of surface coverage enters in two ways. One is in the exponential term, since U_{max} increases with σ, and the other one is through the preexponential factor, $(\alpha L)^{-1}$. In both cases, the effect of surface coverage is to decrease the kinetic coefficient, with the exponential part being much more dominant.

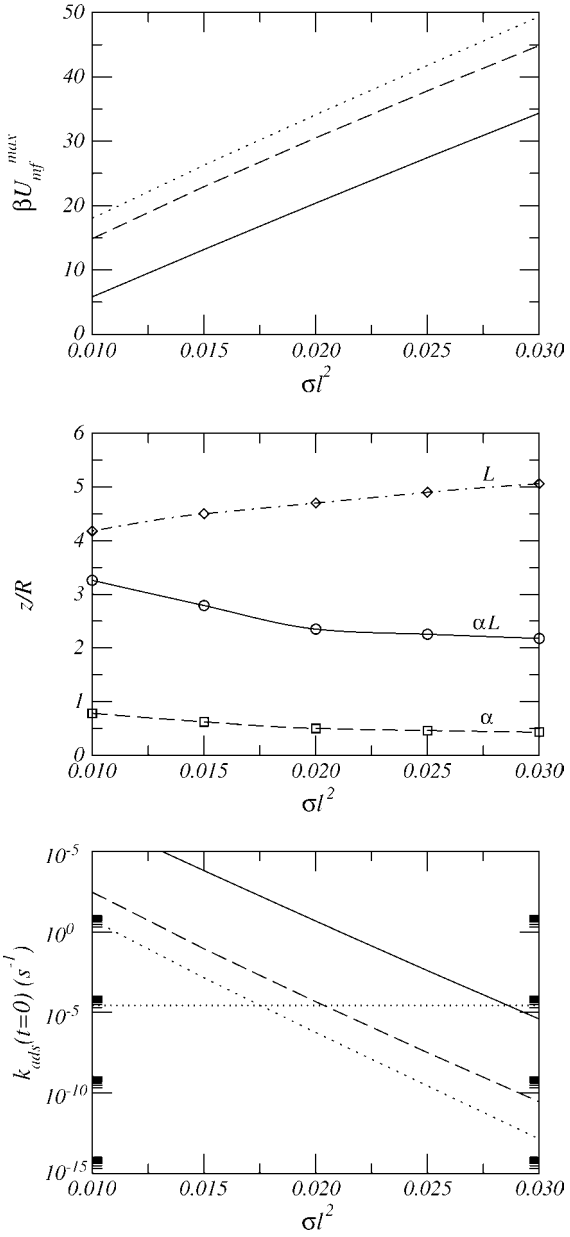

FIGURE 8 (*Top*) The maximum potential of mean-force as a function of surface coverage when no proteins are adsorbed for different chain lengths: $n_g = 50$ (*solid line*), $n_g = 100$ (*long-dashed line*), and $n_g = 150$ (*dotted line*). (*Middle*) The thickness of the grafted polymer layer, L (*dot-dashed line* with *diamonds*), the width of the kinetic barrier, α (*long-dashed line* with *squares*), and the product $L\alpha$ (*solid line* with *circles*), before adsorption as a function of polymer surface coverage for $n_g = 50$. (*Bottom*) The initial rate constant $k_{ads}(t = 0)$ as a function of surface coverage for the three chain lengths shown in the top panel. The thin dotted line marks the rate that corresponds to a time constant of 10 h, i.e., 36,000 s.

The initial rate constants are shown in the bottom graph of Fig. 8 as a function of surface coverage for three polymer chain lengths. There is a very sharp decrease of the constant with surface coverage. The figure also includes a line for a rate that corresponds to a time constant of $\tau = 1/k_{ads} = 10$ h. This is an arbitrary cutoff, but it is shown to demonstrate how, given a desired timescale for prevention of adsorption, one can use the figure as a design tool in terms of the molecular weight and surface coverage necessary to graft on the surface. From the figure, one can see that a longer chain length requires a much smaller surface coverage. Interestingly, if we would use the equilibrium adsorption as a design tool we will need the same surface coverage for the three molecular weights, since the isotherms are independent of molecular weight for the range of chain lengths shown in Fig. 8 (30).

Fig. 9 shows the amount of protein on the surface as a function of time for the desorption process. The starting point of the desorption is the equilibrium achieved under the conditions shown in Fig. 3. The desorption kinetics shown correspond to the cases of surfaces without grafted polymer and a variety of surfaces with grafted polymers of different chain length, all at the same surface coverage. The initial time for desorption is very long in all cases. Further, the timescale for the initial desorption of proteins from the surface is much longer than the initial time for adsorption (compare Fig. 9 with Fig. 3). These results are due mostly to the strong protein-surface attraction upon contact, which leads to strong kinetic barriers for desorption.

Fig. 9 shows a nonmonotonic dependence of the initial time of desorption on polymer-chain length. For very short chain length, increasing the molecular weight of the polymer decreases the initial desorption time; however, for $n_g > 25$, the desorption time increases with increasing molecular weight. There are two effects that may contribute to the nonmonotonic behavior. One is the amount of protein adsorbed before desorption takes place, and the second is the role of the grafted polymer. To understand each of those effects it is convenient to uncouple them. First, we consider the case in which we fix the amount of protein adsorbed, and look at the desorption kinetics for different chain lengths from short to long. This is shown in Fig. 10. The motivation behind this case is to test whether the abnormal behavior for the very

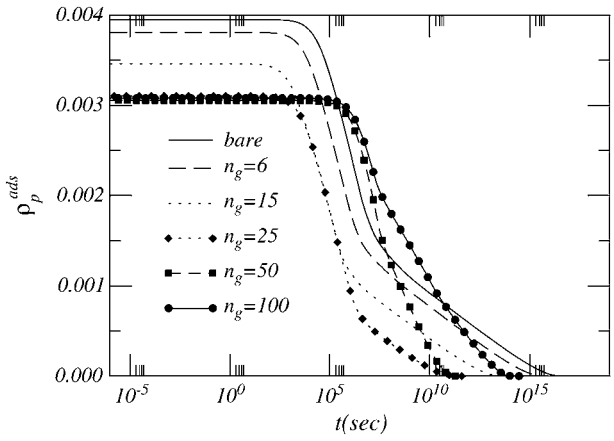

FIGURE 9 The reduction of the density of adsorbed proteins as a function of time for surfaces with grafted polymers of different chain lengths as denoted in the figure. For all chain lengths, the surface coverage of grafted polymer is $\sigma l^2 = 0.01$.

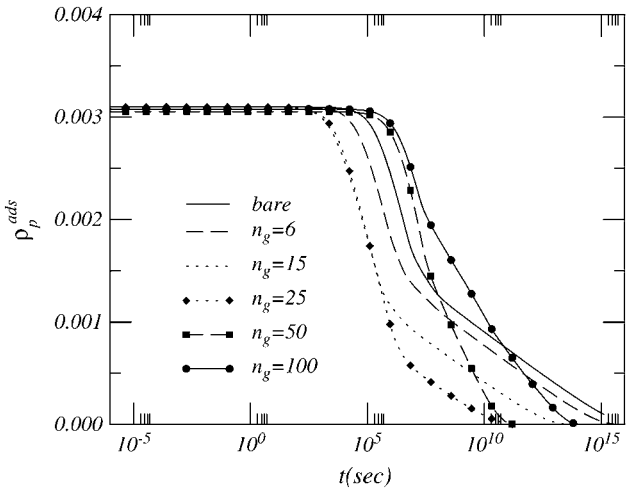

FIGURE 10 The amount of protein on the surface as a function of time during the desorption process for surfaces with grafted polymers with chain length as marked in the figure. The initial amount of protein adsorbed is set to $\rho_p^{ads}(t=0) = 3.1 * 10^{-3}$. For all chain lengths, the surface coverage of grafted polymer is $\sigma l^2 = 0.01$.

short chains shown in Fig. 9 is due to the different initial amount of proteins adsorbed. It is found that the nonmonotonic behavior continues, although the initial number of proteins on the surface is the same for all chain lengths.

Now we focus on the role of the grafted polymer. This effect can be seen in Fig. 11, where we show the volume fraction profiles of short and long chains grafted on surfaces with large and small amounts of proteins adsorbed. All the cases correspond to the same surface coverage of polymer. The two figures for the shortest chain length show that all the

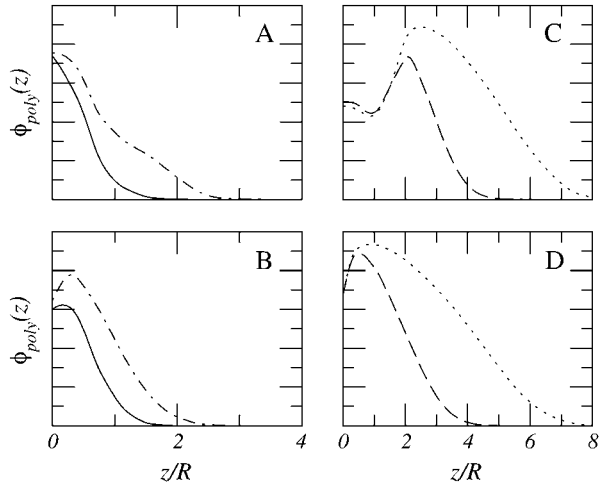

FIGURE 11 The polymer volume fraction profiles for short (*A* and *B*) and longer grafted chains (*C* and *D*). The short chains correspond to $n_g = 15$ (*solid line*) and $n_g = 25$ (*dot-dashed line*), and the longer chains have $n_g = 50$ (*long-dashed line*) and $n_g = 100$ (*dotted line*). *A* and *C* represent cases with a large amount of protein adsorbed, e.g., $\rho_p^{ads} = 3.08\times10^{-3}$. *B* and *D* show cases with a very small amount of protein adsorbed, e.g., $\rho_p^{ads} = 10^{-10}$.

profiles become deformed upon desorption of the proteins, whereas for the longest two chain lengths, the profiles for distances larger than the size of the protein are very similar both with and without proteins adsorbed. That is, all the segments of the short chains interact with the proteins on the surface and play a role in the repulsions responsible for the interactions that determine the desorption. Thus, increasing the length of short chains results in stronger repulsions to facilitate fast desorption—i.e., shorter initial desorption time. However, once the chain length is long enough for the polymer chains to stretch beyond the adsorbed proteins, the segments at distances larger than the protein diameter impose a steric barrier to trap the proteins on the surface. In this situation, increasing the length of long polymer chains leads to a stronger steric barrier to prevent desorption, i.e., longer initial desorption time. As it is the case for the effect of chain length on the equilibrium adsorption isotherms, the crossover chain-length is determined by the ratio between the size of the protein and the polymer layer thickness. Layers with thickness smaller than the protein size show one type of molecular-weight dependence, while those layers with thickness larger than the protein size show a different type.

The results just presented show how the combination of the understanding of the kinetics and equilibrium are important for the best practical design of surface modifiers. Moreover, the results also demonstrate the very different role that surface coverage, and in particular, polymer-chain length, have on the thermodynamics and kinetics of protein adsorption and desorption.

DISCUSSION AND CONCLUSIONS

The kinetics of protein adsorption on surfaces with grafted polymers is a complex process, which is due to the constant change of the layer as proteins adsorb. The flexibility of the chain molecules allows for a deformation of the polymer layer as the adsorption process takes place. This results in time-dependent effective protein-surface interactions that are a function of the amount of proteins adsorbed and the type and amount of polymer grafted on the surface. The timescales for protein adsorption are very large, and many adsorption processes are irreversible for any practical purpose.

To study the kinetics of protein adsorption, we have developed a generalized diffusion approach in which the driving forces for adsorption are the gradients of chemical potentials induced by the presence of the surface. Based on the physical assumption that the timescale for protein adsorption is much longer than the local rearrangement of the polymer chains and the motion of the solvent, the approach assumes a separation of timescales in which, for each spatial configuration of the proteins, the polymers and solvent equilibrate. Thus, we use a molecular theory to calculate the time-dependent free energy from which the gradient of chemical potentials can be calculated. Even within this approximation the equations need to be integrated over more

than 16 orders-of-magnitude and at each time-step the constrained free energy needs to be minimized. In practical terms, this implies that at each time-step a set of coupled nonlinear equations with hundreds of thousand of terms each (the number of used polymer conformations) needs to be solved at each t. Thus, the computational time is prohibitively expensive if one desires to perform systematic studies as a function of polymer chain length, surface coverage, and other important parameters.

From the few cases in which we have completed the full calculation, we have learned that the kinetics of protein adsorption on surfaces with grafted polymers is dominated by the crossing of the large steric barrier presented by the polymer-protein layer. The adsorption process is completed in timescales measured in hours or longer for the cases that we have studied. A very important component that also comes out from the calculations is that the deformation of the polymer layer as proteins adsorb has to be taken into account at all times. The changes in the structure of the polymer layer-adsorbed proteins result in constant changes of the effective potential barrier that the approaching proteins from solution have to cross, in order to adsorb.

Based on the insights learned from the full calculations, we developed a kinetic theory that enables the systematic study of the kinetics of adsorption/desorption. The basic idea is to write pseudo first-order kinetics for adsorption/desorption for a system of two states: adsorbed and bulk. The kinetic rate coefficients depend upon the *time*-dependent potential of mean-force. The coefficients are composed by two factors: a Boltzmann exponent measuring the difference between the potential at the bulk and that of the barrier maximum for the adsorption rate; and the maximum of the barrier and the potential of mean-force at contact with the surface for the desorption rate. The preexponential factor is approximated from a Kramer-like theory adapted from polymer brushes. This factor is determined by the ratio between the diffusion coefficient of the protein and the product of the length that the protein needs to pass to reach the barrier maxima, and the width of the potential of mean-force at k_BT below the maximum. For adsorption, the protein needs to cross a distance proportional to the polymer layer height and for the desorption the distance is the radius of the protein. The explicit dependence of the kinetic behavior on the properties of the polymer layers, e.g., polymer chain length and surface coverage, enter through the potential of mean-force maximum, its value at contact, and the preexponential factors.

The potential of mean-force maxima and at contact, as well as the width of the barrier, are all properties that are time-dependent. The way that we determine the time-dependence variation of these quantities is by calculating the potentials of mean-force as a function of the amount of protein adsorbed, from no-adsorption to the maximum given by the equilibrium amount of adsorption, which we know before the kinetic calculations are carried out. The determination of the potentials of mean-force is straightforward and fast, and thus, once we have all the quantities as a function of protein density, we can integrate the time-dependent equations by plugging in at each time-step the proper (density-determined) potential values. In this way the calculation time is reduced by many orders-of-magnitude, and we can perform systematic studies that are impossible with the full diffusion approach.

The predictions from the approximate kinetic approach are in excellent agreement with those obtained from the full calculations. This is important for two reasons. First, the physical process that is the rate-determining step is indeed crossing of the (time-dependent) barriers. Second, we can have confidence in the approximate kinetic approach and carry out systematic studies with a relatively small amount of computational effort, without losing any of the molecular details involved in the deformation of the polymer layers as the adsorption takes place.

Applying the kinetic approach, we studied the adsorption kinetics as a function of chain length and surface coverage. We find that for relatively high surface coverage and molecular weight of the polymers, in many cases the initial time of adsorption is so large that for any practical purpose there will be no protein adsorption. This is an important result for practical purposes, since equilibrium calculations predict a finite amount of adsorbed proteins; however, because of the slow kinetics, the adsorption is null for any realistic timescale.

One of the most important novel findings in this work relates to the kinetics of desorption. The specific process that we study here is such that the solution in contact with the polymer layer is replaced by pure solvent after the proteins have adsorbed to the surface. Thus, thermodynamic forces will lead to a new equilibrium situation in which all the proteins would leave the surface. We find that the kinetics of desorption depend upon the amount of proteins adsorbed and there is a very strong dependence on polymer molecular-weight and surface coverage. The kinetics of desorption are very slow for all cases studied. This is particularly true once the polymer layer height is larger than the size of the proteins. This is because these long polymers trap the proteins in the surface by presenting a large barrier through the segments, which are a distance from the surface larger than the size of the proteins.

We see that polymer chain length has a very different role when the thickness of the polymer layer formed is larger or smaller than the protein size. This effect is also very different when treating the equilibrium adsorption as compared to the kinetic behavior. For equilibrium adsorption, once the polymer layer thickness is larger than the protein size there is no effect on increasing the polymer chain length. However, for the kinetics of adsorption, the longer the polymer-chain length, the larger the barrier for adsorption, and the range of the repulsive potential. Therefore, for the kinetics of adsorption, increasing polymer-chain length monotonically increases the adsorption time. Furthermore, the role of polymer-chain

length at the initial, intermediate, and final stages of the adsorption, kinetics may change depending on the surface coverage of polymer. At low surface coverages, the initial time for adsorption increases exponentially with polymer-chain length but the adsorption reaches equilibrium in more or less the same timescale for all chain lengths studied. At high surface coverage, the longer the chain length, the slower the adsorption kinetics at all stages of the process.

For the desorption kinetics, the polymer-chain-length dependence is complex. For chain lengths that produce polymer layers whose thicknesses are smaller than the protein size, increasing polymer molecular-weight results in an *increase* of the desorption rate. However, once the layer thickness is larger than the protein size, increasing the polymer-chain length provides a way to *decrease* the desorption rate, by trapping the proteins between the surface and the barrier presented by the polymer segments found at distance from the surface larger than the protein size.

The mechanism of protein trapping can be used in the design of controlled release of proteins from surfaces. Furthermore, this trapping may be responsible for the experimental findings of Shukhishvili and Granick (41) on the adsorption of human serum albumin on polyelectrolyte brushes. In their experiments they showed that the proteins can be trapped in the polymer brush. Although in the experimental case, electrostatic interactions are very important for the initial adsorption of the proteins, the trapping upon weakening of the electrostatic attractions may be due to the same mechanism predicted here for neutral systems. More work is necessary to clarify this point. However, we are now in a position to use the kinetic approach with our theory, including electrostatic interactions (45,44). This work is currently underway.

There are two main issues that need to be addressed as a clear next-step, to be able to generalize the approach to many other, related, systems.

First, what is the role of protein conformational changes in the kinetics of adsorption? We have shown that for the equilibrium isotherms, conformational changes are very important, and the amount and type of adsorbed protein conformer can be controlled by the choice of polymer layer (34). Furthermore, we (33) and others (60) have shown that the kinetics of protein adsorption on surfaces without grafted proteins is very rich and complex whenever conformational changes are explicitly accounted for. Therefore, we are currently generalizing the kinetic approach to study the full kinetic adsorption process on surfaces with grafted polymers and the ability of the proteins to change their conformation upon adsorption.

Second, we have assumed throughout this work that the only relevant inhomogeneous direction is the one normal to the surface. The adsorption process is dominated by barrier crossing, and thus, the lateral arrangement of the polymer-protein mixtures close to the surface may play an important role in lowering the barriers as compared to the quantities calculated in the present work. Preliminary calculations seem to indicate that this is not, in general, the case. However, we are starting to study this effect in detail, to learn under what conditions the approximations used in this work are valid.

Our current understanding of the thermodynamics and kinetic of protein adsorption on surfaces with grafted proteins shows the very large number of ways by which the adsorption process can be controlled. Furthermore, the very good agreement (21,31) between the predictions of the theory and experimental observations suggest that the predictive power of the theory is very good. Therefore, we are developing molecular models for a family of proteins that will enable us to predict their adsorption properties and thus, help in the design of devices for which adsorption plays a major role, such as in electrophoresis, separations, and controlled-release devices. In these models, specific protein-polymer interactions are included and thus we also expect to be able to study the nonmonotonic molecular weight effect found experimentally (47). Moreover, the approach presented here can be applied to studying the adsorption of nanometer-size colloidal particles on surfaces with grafted polymers. We are already studying these types of systems, particularly for charged particles adsorbing on polyelectrolyte-grafted layers (61).

APPENDIX

Numerical method

The numerical solution of the minimization of the free-energy functional is obtained by discretization of the z direction into parallel layers of thickness δ. Define the i^{th} layer as the region between $(i-1)\delta \le z < i\delta$. The packing constraint, Eq. 6, in discrete form is

$$\sigma \sum_{\{\gamma\}} P_{\text{g}}(\gamma) v_{\text{g}}(\gamma; i) + \sum_{\text{j=1}}^{\{\text{i<M:i,M}\}} \{[\rho_{\text{p}}(i-j+1)v_{\text{s}}]v_{\text{p}}(j)\} + \phi_{\text{s}}(i) = 1, \tag{22}$$

where $\{i<M{:}i, M\}$ means if $i < M$, the upper limit for j is i; otherwise, it is M. The term M is the number of layers a protein molecule spans in the discretized space, i.e., $M = 2R/\delta$. Further, the sum over γ is over the number of conformations that we generate to model the polymer chains.

Eqs. 9, 7, and 8 in discrete form are given by

$$\phi_{\text{s}}(i) = e^{-\beta\pi(\text{i})v_{\text{s}}}, \tag{23}$$

$$P_{\text{g}}(\gamma) = \frac{1}{q_{\text{g}}} e^{-\sum_{\text{i=1}}^{\text{i}_{\text{Max}}} [\beta\pi(\text{i})v_{\text{s}}]v_{\text{g}}(\gamma;\text{i})/v_{\text{s}}}, \tag{24}$$

and

$$\rho_{\text{p}}(i) = e^{\beta\mu_{\text{p}}^{\text{bulk}}} e^{-\beta U_{\text{mf}}(\text{i})}, \tag{25}$$

with (from Eq. 11)

$$\beta U_{\text{mf}}(i) = \beta U_{\text{ps}}(i) + \sum_{\text{j=1}}^{\text{M}} [\beta\pi(i+j-1)v_{\text{s}}] * \frac{v_{\text{p}}(j)}{v_{\text{s}}}. \tag{26}$$

We define $x(i) = e^{-\beta\pi(i)v_s}$ where $1 \le i \le i_{Max}$ (i_{Max} is the total number of layers considered in the system). Then, substituting Eqs. 23–26 into Eq. 22 transforms the packing constraint into functions of $x(i)$. Then we solve the i_{Max} coupled nonlinear equations for $x(i)$ by standard numerical methods. Once $x(i)$ for all i are known, we can calculate any desired equilibrium average quantity. More details can be found in Fang and Szleifer (34).

Derivation of rate coefficient for the adsorption process

The chemical potential of a protein at z is

$$\beta\mu_p(z) = ln\,\rho_p(z) + \beta U_{mf}(z). \tag{27}$$

The gradient of chemical potential induces a flux, $J(z) = \rho_p(z)v(z)$, leading to a uniform and constant chemical potential everywhere at equilibrium. The average velocity of this flux $v(z)$ is

$$v(z) = -D\frac{\partial\beta\mu_p(z)}{\partial z}, \tag{28}$$

where D is the diffusion coefficient. The corresponding flux is

$$\begin{aligned} J(z) &= -D\rho_p(z)\frac{\partial\beta\mu_p(z)}{\partial z} \\ &= -D\rho_p(z)\frac{\beta U_{mf}(z)}{\partial z} - D\frac{\partial\rho_p(z)}{\partial z} \\ &= -De^{-\beta U_{mf}(z)}\frac{\partial}{\partial z}[\rho_p(z)e^{\beta U_{mf}(z)}]. \end{aligned} \tag{29}$$

This is the starting point for the high-viscosity limit of the Kramer's rate theory (48). It involves a steady-state solution, $J(z) = constant$, representing, in our case, a stationary one-dimensional net flux from the bulk to the surface. (Note that in Halperin's article—see Ref. 48—he focuses on the initial adsorption and only considers the protein flux from the bulk to the surface. This is because initially when there are no proteins adsorbed, no flux flows out of the surface. Here we extend Halperin's idea to study the whole kinetic process and consider the net flux, i.e., the sum of the inflow flux and the outflow flux. For the adsorption process, we assume the net flux is always toward the surface.) Apply the steady-state assumption, i.e., $J(z) = j$ and rewrite Eq. 29 as

$$je^{\beta U_{mf}(z)}dz = -Dd[\rho_p(z)e^{\beta U_{mf}(z)}]. \tag{30}$$

Integrating both sides of Eq. 30 from the surface, i.e., $z = 0$, to the boundary of the polymer layer, i.e., $z = L_0$, which corresponds to the bulk solution of the proteins, yields

$$j\int_0^{L_0} e^{\beta U_{mf}(z)}dz = -D\left[\rho_p^{bulk}e^{\beta U_{mf}^{bulk}} - \rho_p^{ads}\,e^{\beta U_{mf}(0)}\right]. \tag{31}$$

The integral on the left side of Eq. 31 is approximately evaluated by expanding $U_{mf}(z)$ around its maximum, i.e., U_{mf}^{max}, at z^* (48). Namely, $U_{mf}(z) = U_{mf}^{max} - (\omega/2)(z-z*)^2$, where we neglect the terms beyond second-order and ω is the curvature of the potential of mean-force at z^*. Thus, the integral becomes $e^{\beta U_{mf}^{max}}\int_0^{L_0} e^{-(\beta\omega/2)(z-z^*)^2}dz$. Since the integral is dominated by the contribution from $z = z^*$, for simplicity, we may extend the integration limit to $\pm\infty$ and get $(2\pi kT/\omega)^{1/2}$. In turn, the width of the barrier kT below U_{mf}^{max}, α, is $kT/\omega = \alpha^2$ (48). As a result, the steady-state flux is

$$j \approx -(2\pi)^{-1/2}\frac{D}{\alpha}\left\{e^{-\left[\beta U_{mf}^{max}-\beta U_{mf}^{bulk}\right]}\rho_p^{bulk} - e^{-\left[\beta U_{mf}^{max}-\beta U_{mf}(0)\right]}\rho_p^{ads}\right\}. \tag{32}$$

One point to clarify is that of the steady-state flux (which we assume is constant for all z at any time t). The constants for different t may actually be different. Furthermore, we assume that the steady-state flux for different t changes continuously with t. According to Einstein's diffusion relation $Dt_1 \approx \alpha^2$, where t_1 is the characteristic time to diffuse across the barrier, $D/\alpha(= \alpha/t_1)$ is the diffusion rate across the barrier. The Boltzmann factor, $e^{-[\beta U_{mf}^{max}-\beta U_{mf}^{bulk}]}$, accounts for the probability for particles in the bulk to reach the peak of the barrier and $e^{-[\beta U_{mf}^{max}-\beta U_{mf}(0)]}$ is the probability that the particles on the surface jump to the peak of the potential barrier. Considering the net flux flowing from the bulk to the surface, we have

$$j = \rho_p^{bulk}v_{flux}, \tag{33}$$

where

$$v_{flux} \approx -\frac{D}{\alpha}\left\{e^{-\left[\beta U_{mf}^{max}-\beta U_{mf}^{bulk}\right]} - e^{-\left[\beta U_{mf}^{max}-\beta U_{mf}(0)\right]}\frac{\rho_p^{ads}}{\rho_p^{bulk}}\right\} \tag{34}$$

is the net flux velocity to cross the barrier. The time to cross a barrier of overall thickness L is L/v_{flux} and the rate coefficient for the adsorption process is expressed as

$$k_{ads} = \frac{D}{\alpha L}\left\{e^{-\left[\beta U_{mf}^{max}-\beta U_{mf}^{bulk}\right]} - e^{-\left[\beta U_{mf}^{max}-\beta U_{mf}(0)\right]}\frac{\rho_p^{ads}}{\rho_p^{bulk}}\right\}, \tag{35}$$

and the rate of adsorption is defined as

$$\frac{d\rho_p^{ads}}{dt} = k_{ads}\rho_p^{bulk}. \tag{36}$$

That is,

$$\frac{d\rho_p^{ads}}{dt} = \frac{D}{\alpha L}e^{-\left[\beta U_{mf}^{max}-\beta U_{mf}^{bulk}\right]}\rho_p^{bulk} - \frac{D}{\alpha L}e^{-\left[\beta U_{mf}^{max}-\beta U_{mf}(0)\right]}\rho_p^{ads}. \tag{37}$$

Note that this expression fulfills microscopic reversibility at all times. This is in line with the basic approximation in our approach that the system is in local thermodynamic equilibrium and with the separation of timescales. However, due to this condition, we obtain that $k_1 = k_2 = D/\alpha L$ (see Eqs. 18 and 37), which seems counterintuitive—since the distance that the protein has to travel to reach the maximum is not the same when coming from the solution or from the surface. However, this is the result of considering the total flux toward the surface in the adsorption process. Moreover, other choices for the preexponential factor do not change the presented results for the kinetics of adsorption. Therefore, this choice of preexponential coefficients is justified for two reasons. First, the flux in all adsorption processes of interest is toward the surface; and second, the comparisons of the predictions of the KA with the full GDA are in excellent agreement (see Fig. 3). In the case of desorption, a different preexponential factor is obtained, as derived next.

Derivation of rate coefficient for the desorption process

The steady-state flux for the desorption process is

$$j \approx \frac{D}{\alpha}e^{-\left[\beta U_{mf}^{max}-\beta U_{mf}(0)\right]}\rho_p^{ads}, \tag{38}$$

which is obtained from Eq. 32 by setting $\rho_p^{bulk} = 0$. Note that for the desorption process, the flux is a stationary one-dimensional flux from the surface to the bulk. This means that the flux will cross the barrier from the surface side rather than from the bulk side, as in the case for the adsorption process. On the surface

$$j = \rho_p^{ads} v_{flux}, \tag{39}$$

and the flux velocity to cross the barrier is thus

$$v_{flux} \approx \frac{D}{\alpha} e^{-\left[\beta U_{mf}^{max} - \beta U_{mf}(0)\right]}. \tag{40}$$

In most cases the kinetic barrier moves toward the surface as the adsorption reaches equilibrium. Therefore, the relevant thickness that the protein needs to move to reach the barrier is of the order of the size of the protein, i.e., $L \sim R$. That is, the thickness of the polymer layer is not so important for the desorption kinetics as for the adsorption kinetics. The rate coefficient for the desorption process is thus v_{flux}/R, i.e.,

$$k_{des} = \frac{D}{\alpha R} e^{-\left[\beta U_{mf}^{max} - \beta U_{mf}(0)\right]}, \tag{41}$$

and the rate equation to be solved is

$$\frac{d\rho_p^{ads}}{dt} = -k_{des}\rho_p^{ads}. \tag{42}$$

We thank Dr. Marcelo Carignano for insightful discussions throughout the different stages of this work.

This material is based upon work supported by the National Science Foundation under grant No. CTS-0338377, and by the Indiana 21st Century Fund.

REFERENCES

1. Milner, S. T. 1991. Polymer brushes. *Science*. 251:905–914.
2. Halperin, A., M. Tirrell, and T. Lodge. 1992. Tethered chains in polymer microstructures. *Adv. Polym. Sci.* 100:31–71.
3. Szleifer, I., and M. A. Carignano. 1996. Tethered polymer layers. *Adv. Chem. Phys*. 44:165–260.
4. Napper, H. D., editor. 1993. Polymeric Stabilization of Colloidal Dispersions. Academic Press, Orlando, FL.
5. Israelachvili, J. 1991. Intermolecular and Surface Forces. Academic Press, Orlando, FL.
6. Evans, D., and H. Wennestrom. 1998. The Colloidal Domain: Where Physics, Chemistry and Biology Meet. John Wiley and Sons, New York.
7. McPherson, T. B., S. J. Lee, and K. Park. 1995. Analysis of the prevention of protein adsorption by steric repulsion theory. *ACS Symp. Series.* 602:395–404.
8. Woodle, M. C. 1997. Poly(ethylene glycol)-grafted liposome therapeutics. *ACS Symp. Series*. 680:60–81.
9. Gabizon, A. A. 1995. Liposome circulation time and tumor targeting: implications for cancer chemotherapy. *Adv. Drug Deliv. Rev*. 16:285–294.
10. Gref, R., A. Domb, P. Quellec, T. Blunk, R. H. Muller, J. M. Verbavatz, and R. Langer. 1995. The controlled intravenous delivery of drugs using PEG-coated sterically stabilized nanospheres. *Adv. Drug Deliv. Rev*. 16:215–233.
11. Mosqueira, V. C. F., P. Legrand, A. Gulik, O. Bourdon, R. Gref, D. Labarre, and G. Barratt. 2001. Relationship between complement activation, cellular uptake and surface physicochemical aspects of novel PEG-modified nanocapsules. *Biomaterials*. 22:2967–2979.
12. Chen, Z., R. Ward, Y. Tian, F. Malizia, D. H. Gracias, Y. R. Shen, and G. A. Somorjai. 2002. Interaction of fibrinogen with surfaces of end-group-modified polyurethanes: a surface-specific sum-frequency-generation vibrational spectroscopy study. *J. Biomed. Mater. Res.* 62:254–264.
13. Kawano, H., K. Kurita, Y. Iwasaki, K. Ishihara, and N. Nakabayashi. 1998. Blood compatibility of cellulose hemodialysis membrane grafted with various polymers. *Kobunshi Ronbunshu.* 55:334–343.
14. Iwasaki, Y., N. Nakabayashi, and K. Ishihara. 2001. Preservation of platelet function on 2-methacryloyloxyethyl phosphorylcholine-graft polymer as compared to various water-soluble graft polymers. *J. Biomed. Mater. Res*. 57:72–78.
15. Kim, J. H., and S. C. Kim. 2002. PEO-grafting on PU/PS IPNS for enhanced blood compatibility—effect of pendant length and grafting density. *Biomaterials*. 23:2015–2025.
16. Sofia, S. J., V. Premnath, and E. W. Merrill. 1998. Poly(ethylene oxide) grafted to silicon surfaces: grafting density and protein adsorption. *Macromolecules*. 31:5059–5070.
17. Malmsten, M., K. Emoto, and J. M. V. Alstine. 1998. Effect of chain density on inhibition of protein adsorption by poly(ethylene glycol) based coatings. *J. Colloid Interface Sci.* 202:507–517.
18. Lee, J. H., B. J. Jeong, and H. B. Lee. 1997. Plasma protein adsorption and platelet adhesion onto comb-like PEO gradient surfaces. *J. Biomed. Mater. Res.* 34:105–114.
19. Qiu, Y. X., D. Klee, W. Pluster, B. Severich, and H. Hocker. 1996. Surface modification of polyurethane by plasma-induced graft polymerization of poly(ethylene glycol) methacrylate. *J. Appl. Polym. Sci.* 61:2373–2382.
20. Emoto, K., J. M. Harris, and J. M. V. Alstine. 1996. Grafting poly(ethylene glycol) epoxide to amino-derivatized quartz: effect of temperature and pH on grafting density. *Anal. Chem.* 68:3751–3757.
21. McPherson, T., A. Kidane, I. Szleifer, and K. Park. 1998. Prevention of protein adsorption by tethered poly(ethylene oxide) layers: experiments and single-chain mean-field analysis. *Langmuir*. 14:176–186.
22. Lee, H. J., K. D. Park, H. D. Park, W. K. Lee, D. K. Han, S. H. Kim, and Y. H. Kim. 2000. Platelet and bacterial repellence on sulfonated poly(ethylene glycol)-acrylate copolymer surfaces. *Colloid Surface B*. 18:355–370.
23. Gombotz, W. R., W. Guanghui, T. A. Horbett, and A. S. Hoffman. 1991. Protein adsorption to poly(ethylene oxide) surfaces. *J. Biomed. Mater. Res*. 25:1547–1562.
24. Szleifer, I. 1997. Polymers and proteins: interactions at interfaces. *Curr. Opin. Solid St. Mat. Sci.* 2:337–344.
25. Lasic, D. , and F. Martin, editors. 1995. Stealth Liposomes. CRC Press, Boca Raton, FL.
26. Tan, J. S., and P. A. Martic. 1990. Protein adsorption and conformational change on small polymer particles. *J. Colloid Interface Sci.* 136: 415–431.
27. Bartucci, R., M. Pantusa, D. Marsh, and L. Sportelli. 2002. Interaction of human serum albumin with membranes containing polymer-grafted lipids: spin-label ESR studies in the mushroom and brush regimes. *BBA Biomembr*. 1564:237–242.
28. Snellings, G. M. B. F., S. O. Vansteenkiste, S. I. Corneillie, M. C. Davies, and E. H. Schacht. 2000. Protein adhesion at poly(ethylene glycol) modified surface. *Adv. Mater.* 12:1959–1962.
29. Moribe, K., K. Maruyama, and M. Iwatsuru. 1997. Estimation of surface state of poly(ethylene glycol)-coated liposomes using an aqueous two-phase partitioning technique. *Chem. Pharm. Bull*. (*Tokyo*). 45: 1683–1687.
30. Szleifer, I. 1997b. Protein adsorption on surface with grafted polymers: a theoretical approach. *Biophys. J*. 72:595–612.
31. Satulovsky, J., M. A. Carignano, and I. Szleifer. 2000. Kinetic and thermodynamic control of protein adsorption. *Proc. Natl. Acad. Sci. USA*. 97:9037–9041.
32. Szleifer, I., and M. A. Carignano. 2000. Tethered polymer layers: phase transitions and reduction of protein adsorption. *Macromol. Rapid Comm.* 21:423–448.
33. Fang, F., and I. Szleifer. 2001. Kinetics and thermodynamics of protein adsorption: a generalized molecular theoretical approach. *Biophys. J*. 80:2568–2589.
34. Fang, F., and I. Szleifer. 2002. Effect of molecular structure on the adsorption of protein on surfaces with grafted polymers. *Langmuir*. 18:5497–5510.

35. Lee, S. J., and K. Park. 1994. Protein interaction with surfaces: separation distance-dependent interaction energies. *J. Vac. Sci. Technol.* 12:1–7.

36. Billsten, P., M. Wahlgren, T. Arnebrant, J. Mcguire, and H. Elwing. 1995. Structural-changes of t4 lysozyme upon adsorption to silica nanoparticles measured by circular-dichroism. *J. Colloid Interface Sci.* 175:77–82.

37. Steadman, B. L., K. C. Thompson, C. R. Middaugh, K. Matsuno, S. Vrona, E. Q. Lawson, and R. V. Lewis. 1992. The effects of surface-adsorption on the thermal-stability of proteins. *Biotechnol. Bioeng.* 40:8–15.

38. Buijs, J., and V. Hlady. 1997. Adsorption kinetics, conformation, and mobility of the growth hormone and lysozyme on solid surfaces, studied with TIRF. *J. Colloid Interface Sci.* 190:171–181.

39. Feder, J., and I. Giaever. 1980. Adsorption of ferritin. *J. Colloid Interface Sci.* 78:144–154.

40. Schaaf, P., and J. Talbot. 1989. Surface exclusion effects in adsorption processes. *J. Chem. Phys.* 91:4401–4409.

41. Sukhishvili, S. A., and S. Granick. 1999. Adsorption of human serum albumin: dependence on molecular architecture of the oppositely charged surface. *J. Chem. Phys.* 110:10153–10161.

42. Szleifer, I. 1997c. Protein adsorption on tethered polymer layers: effect of polymer chain architecture and composition. *Physica A* (*Amsterdam*). 244:370–388.

43. Carignano, M. A., and I. Szleifer. 2000. Prevention of protein adsorption by flexible and rigid chain molecules. *Colloid Surface B.* 18: 169–182.

44. Carignano, M. A., and I. Szleifer. 2002. Adsorption of model charged proteins on charged surfaces with grafted polymers. *Mol. Phys.* 100: 2993–3003.

45. Fang, F., and I. Szleifer. 2003. Competitive adsorption in model charged protein mixtures: equilibrium isotherms and kinetics behavior. *J. Chem. Phys.* 119:1053–1065.

46. Ostuni, E., R. G. Chapman, R. E. Holmlin, S. Takayama, and G. M. Whitesides. 2001. A survey of structure-property relationships of surfaces that resist the adsorption of protein. *Langmuir.* 17:5605–5620.

47. Norde, W., and D. Gage. 2004. Interaction of bovine serum albumin and human blood plasma with PEO-tethered surfaces: influence of PEO chain length, grafting density, and temperature. *Langmuir.* 20:4162–4167.

48. Halperin, A. 1999. Polymer brushes that resist adsorption of model proteins: design parameters. *Langmuir.* 15:2525–2533.

49. Fraaije, J. G. E. M. 1993. Dynamic density functional theory for microphase separation kinetics of block copolymer melts. *J. Chem. Phys.* 99:9202–9212.

50. Hasegawa, R., and M. Doi. 1997. Adsorption dynamics. extension of self-consistent field theory to dynamical problems. *Macromolecules.* 30:3086–3089.

51. Marconi, U. M. B., and P. Tarazona. 1999. Dynamic density functional theory of fluids. *J. Chem. Phys.* 110:8032–8044.

52. Chandler, D. 1987. Introduction to Modern Statistical Mechanics. Oxford University Press, New York.

53. Kondepudi, D., and I. Prigogine. 1998. Modern Thermodynamics: From Heat Engines to Dissipative Structures. John Wiley and Sons, New York.

54. Carignano, M. A., and I. Szleifer. 1993. Statistical thermodynamical theory of grafted polymeric layers. *J. Chem. Phys.* 98:5006–5018.

55. Carignano, M. A., and I. Szleifer. 1995a. On the structure and lateral pressures of tethered polymer layers in good solvent. *Macromolecules.* 28:3205–3213.

56. Carignano, M. A., and I. Szleifer. 1995b. Structural and thermodynamic properties of end-grafted polymers on curved surfaces. *J. Chem. Phys.* 102:8662–8669.

57. Szleifer, I. 1996. Statistical thermodynamics of polymers near surfaces. *Curr. Opin. Colloid Interface Sci.* 1:416–423.

58. Flory, P. J. 1989. Statistical Mechanics of Chain Molecules. Hanser Publishers, Munich, Germany.

59. Faure, M., P. Bassereau, M. Carignano, I. Szleifer, Y. Gallot, and D. Andelman. 1998. Monolayers of diblock copolymer at the air-water interface: the attractive monomer-surface case. *Eur. Phys. J. B.* 3:365–375.

60. Tassel, P. R. V., L. Guemouri, J. J. Ramsden, G. Tarjus, P. Viot, and J. Talbot. 1998. A particle-level model of irreversible protein adsorption with a postadsorption transition. *J. Colloid Interface Sci.* 207:317–323.

61. Wu, T., J. Genzer, P. Gong, I. Szleifer, P. Vlček, and V. Subr. 2004. Behavior of surface-anchored poly(acrylic acid) brushes with grafting density gradients on solid substrates. *In* Polymer Brushes. R. Advincula, W. Brittain, K. Caster, and J. Rüen, editors. Willey-VCH, Weinheim, Germany. 287–315.